Miah, Md Suzan; Icheln, Clemens; Islam, Md Mazidul; Haneda, Katsuyuki

An Ultrawideband Conformal Antenna at 433 MHz for Wireless Capsule Endoscope of Pediatric Patients

Published in:
2018 IEEE 29th Annual International Symposium on Personal, Indoor and Mobile Radio Communications, PIMRC 2018

DOI:
10.1109/PIMRC.2018.8580890

Published: 18/12/2018

Document Version
Peer-reviewed accepted author manuscript, also known as Final accepted manuscript or Post-print

Please cite the original version:
Miah, M. S., Icheln, C., Islam, M. M., & Haneda, K. (2018). An Ultrawideband Conformal Antenna at 433 MHz for Wireless Capsule Endoscope of Pediatric Patients. In *2018 IEEE 29th Annual International Symposium on Personal, Indoor and Mobile Radio Communications, PIMRC 2018* (Vol. 2018-September, pp. 350-355). Article 8580890 (IEEE International Symposium on Personal, Indoor, and Mobile Radio Communications workshops). IEEE. https://doi.org/10.1109/PIMRC.2018.8580890

An Ultrawideband Conformal Antenna at 433 MHz for Wireless Capsule Endoscope of Pediatric Patients

Md. Suzan Miah, Clemens Icheln, Md. Mazidul Islam, and Katsuyuki Haneda
Aalto University School of Electrical Engineering, Espoo, Finland
Email: md.miah@aalto.fi

***Abstract*—Wireless capsule endoscopy (WCE) systems are used to capture images of the human digestive tract for medical applications. The antenna is one of the most important components in a WCE system. In this paper, we propose a compact capsule antenna operating at the 433-MHz ISM band. The antenna conforms to the outer-wall of a small capsule module with dimensions of 19.5 mm $\times$ 10 mm. A colon-equivalent tissue phantom and CST Gustav voxel human body model were used to numerically verify the operation of the capsule antenna. The simulation results in the colon-tissue phantom were then validated through *in-vitro* measurements using a liquid phantom. According to the phantom simulations, the capsule antenna has -10 dB impedance matching from 288 to 2200 MHz. The ultrawideband characteristic enables the capsule antenna to tolerate the detuning effects due to electronic modules in the capsule and due to the proximity of various different tissues in gastrointestinal tracts. While providing ultrawide operational bandwidth and sufficient radiation performance, the small size makes the antenna suitable especially for pediatric patients in addition to adults.**

I. Introduction

Wireless capsule endoscopy (WCE) is used to record images of the digestive tract for medical applications [1]. One of the use cases of capsule endoscopy is to examine areas of the small intestine that cannot be reached by conventional types of endoscopy. Also, traditional techniques are painful for the patient, whereas WCE is non-invasive and painless. Current devices have dimensions of approximately 26 mm $\times$ 11 mm and are used for both adult and children patients. Thanks to the advanced microelectronics and sensor technology, overall capsule size can be largely reduced, whereas the size of the antenna, which is an important component, remains a challenge. The paper [2] proposes the frequency band $400-600$ MHz for WCE systems because of relatively small propagation losses in the human body. The resonance length of the antenna, which is significantly larger than the capsule size, makes the design of miniaturized antennas at these frequency band challenging.

Recent research activities on capsule antennas have shown embedded [3]–[5] and conformal structures [6]–[18] as promising antenna design strategy. Embedded antennas are placed inside the capsule cavity. The conformal structure utilizes only the surface of the capsule module and leaves the interior for other components, allowing the most effective use of available surface area of a capsule and the antenna as large as possible for better radiation performance [17]. Several wideband conformal antenna designs for WCE systems, operating at frequencies up to 1400 MHz have been reported in literature [6]–[18]. Almost all assume a capsule size of $24-30$ mm in length and $10-12$ mm in diameter. The conformal antenna in [14]–[16] report -10 dB impedance matching bandwidth ($\mathrm{BW}_{-10\mathrm{dB}}$) of 200 MHz, whereas in [7] $\mathrm{BW}_{-10\mathrm{dB}} = 20$ MHz. In [8], an outer-wall conformal microstrip antenna is proposed with $\mathrm{BW}_{-10\mathrm{dB}} = 39.9$ MHz, while the microstrip antenna in [9] reaches $\mathrm{BW}_{-10\mathrm{dB}} = 50$ MHz. A patch with $\mathrm{BW}_{-10\mathrm{dB}} = 124.4$ MHz is reported in [11], while a conformal meandered arm dipole reaches $\mathrm{BW}_{-10\mathrm{dB}} = 158$ MHz in [12]. The loop antenna reported in [17] works at center frequency of 500 MHz with $\mathrm{BW}_{-10\mathrm{dB}} = 260$ MHz. Another outer-wall loop antenna with $\mathrm{BW}_{-10\mathrm{dB}} = 785$ MHz is reported in [18] but without experimental validation. In the authors' own work [19], a conformal antenna reports a maximum $\mathrm{BW}_{-10\mathrm{dB}}$ of 795 MHz. A more complete comparison of these references is shown in Table 1.

According to the studies reported in [20], current devices are relatively large for children to swallow. Similarly, [21] shows that 11% of children were even unable to swallow such a capsule. In order to make such WCE system suitable for pediatric applications, the overall size of the capsule should be reduced. In addition to the requirement of miniaturization, the bandwidth of the antenna needs to be as wide as possible to overcome the detuning effects due to varying tissue properties through the digestive tract, as well as to realize higher data rates. According to the author's best knowledge, the smallest capsule antenna is reported for a capsule with a size of only 17 mm $\times$ 7 mm in [6] and [10], but the $\mathrm{BW}_{-10\mathrm{dB}}$ is only 17 MHz and 53 MHz, respectively. Keeping in mind the operation environment of a WCE system, these matching bandwidths are relatively narrow.

Since a standard size of the capsule for pediatric patients is not defined yet, main design requirement of a capsule antenna is that it should have wider matching bandwidth with a same or smaller capsule size than the existing designs. In this paper, we propose an ultrawideband conformal loop antenna attached on the outer-wall of a capsule module with the size of 19.5 mm $\times$ 10 mm operating at 433 MHz industrial, scientific and medical (ISM) band. The simulation results show that proposed antenna has a $\text{BW}_{-10\text{dB}}$ of 1912 MHz (288-2200 MHz), which is a much wider than reported existing designs, and allows a much smaller capsule size except for that in [6], [10]. It was also demonstrated that the proposed antenna is robust against changes of surrounding environments such as other components in the capsule, different tissues in the digestive tract, different locations, and varying orientations inside the body.

The remainder of this paper is organized as follows. Section II illustrates the proposed capsule antenna configuration and simulations, while Section III addresses the experimental validation of the numerical results. Finally, Section IV concludes this paper.

II. Capsule Antenna Design and Simulations

A. Antenna Structure

The proposed antenna is a loop antenna patterned on a 100 μm thick flexible substrate Preperm 255 with relative permittivity, ε_{r}, and loss tangent, $\tan\delta$ of 2.55 and 5.0×10^{-4}, respectively. The flexible substrate allows the antenna to be wrapped around the capsule. The proposed antenna before and after wrapping it around the capsule is shown in Fig. 1(a) and Fig. 1(b), respectively. The antenna occupies the outer-wall of the cylinder and one side of a dome of the capsule module, whereas other remains free for optical components and camera. The capsule module is made of polystyrene with $\varepsilon_{\text{r}} = 2.6$ and $\tan\delta = 0.05$ at 1 GHz. The thickness of the capsules' wall, diameter, and length of the capsule are 0.5 mm, 10 mm and 19.5 mm, respectively. After wrapping the antenna on the outer wall of the capsule module, the points A and B in Fig. 1(a) were connected at the top of the capsule dome to complete the loop. The feeding point of the antenna in the simulations is indicated by a red triangle in Fig. 1.

B. Capsule Implementation and Detuning Factors Analysis

In simulations, the surrounded medium of the capsule is set to homogeneous colon-tissue equivalent material with the electrical properties of $\varepsilon_{\text{r}} = 62$ and conductivity, $\sigma = 0.87$ at 433 MHz. The simulation was performed using CST Microwave Studio 2018. The X-oriented capsule without biocompatible layer and electronic components in the module was placed at the center of the colon-tissue phantom as shown in Fig. 2. Note that X-oriented means the longest dimension of the capsule is

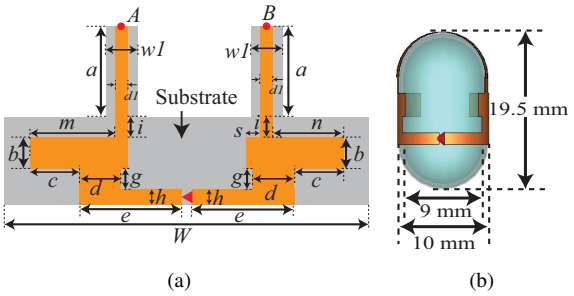

Fig. 1. Capsule antenna (a) before, and (b) after placing around the capsule. The optimized dimensions are (in mm): $a = 7.85$, $b = 3$, $c = 4.75$, $d = 4$, $e = 9.8$, $g = 2$, $h = 1.5$, $i = 2$, $m = 8.2$, $n = 7.35$, $d1 = 1.2$, $w1 = 2.2$, $s = 0.85$, and $W = 31.4$.

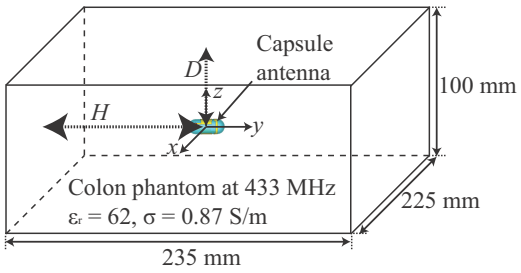

Fig. 2. The antenna arrangement in Fig. 1(b) was implanted in the colon-tissue phantom.

aligned along the X-axis. Fig. 3(a) shows the simulated magnitude of a reflection coefficient, $|S_{11}|$. The antenna has two modes of resonance, one at 420 MHz and another one at 1225 MHz. The antenna shows ultrawideband matching the $|S_{11}| = -10$ dB is achieved across 288 MHz to 2200 MHz. The realized gain of the antenna is -34.5 dBi at 433 MHz, whereas radiation efficiency is -38 dB (0.016%). Since antenna operates inside the very lossy medium, the low radiation efficiency is expected.The remaining part of this subsection includes the studies of detuning of the antenna resonance due to several factors such as orientations and locations of the capsule, as well as electronics inside the module.

1) Biocompatible layer: We started the studies of detuning factors to the antenna resonance by implementing a thin layer of biocompatible material around the capsule. Since the antenna is made of non-biocompatible material and utilizes the outer-wall of the capsule, it is inevitable to use a biocompatible material layer around the capsule to ensure that the antennas' material does not cause any toxic reactions, effects, or injuries in the human body. For this purpose, an X-oriented capsule antenna with 0.1 mm thick Polyamide layer ($\varepsilon_{\text{r}} = 4.3$ and $\tan\delta = 0.004$), which is one of the popular biocompatible materials was simulated at the center of the colon-tissue phantom. A comparison of $|S_{11}|$ of the capsule antenna with and without biocompatible layer is shown in Fig. 3(a). As expected, the resonance of the antenna with the biocompatible layer is slightly up in frequency, because of lower dielectric loading effect than

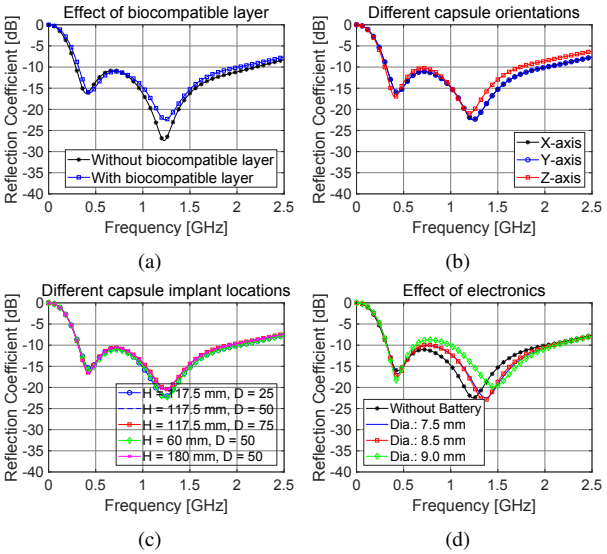

Fig. 3. Detuning effects of capsule antenna matching at the center of the homogeneous colon-tissue phantom as in Fig. 2 due to (a) biocompatible material, (b) capsule orientations, (c) capsule locations, and (d) batteries inside the capsule.

the bare antenna. However, $\text{BW}_{-10\text{dB}}$ remains almost same as in the case of without biocompatible layer. Note that antenna with the biocompatible layer is considered in the sensitivity analysis in the remaining part of this section.

2) Capsule orientation: It is impossible to control the orientation of the capsule. Therefore, the orientation of the capsule is considered random. We numerically evaluate the changes of antenna matching for three different orientations of the capsule at the center of the colon-tissue phantom in Fig. 2. The simulated $|S_{11}|$ for X-, Y- and Z-oriented capsule is presented in Fig. 3(b). The results demonstrate a slight variation of the matching across different orientations. However, -10 dB matching is maintained across wide frequency range for all three cases. Furthermore, we studied the detuning of the antenna's resonance frequencies at different locations within the phantom. The antenna implant depth, D, was first changed along Z-axis from top to bottom while maintaining H = 117.5 mm from the left wall of the phantom, as shown in Fig. 2. Similarly, the antenna location, H, was changed along Y-axis, while maintaining D = 50 mm. The simulated $|S_{11}|$ are presented in Fig. 3(c), showing that they are quite stable for all the tested locations.

3) Electronic components inside a capsule: The endoscopy capsule should contain several electronic components, such as illuminating light, telemetry unit, camera, printed circuit board (PCB), and battery. These components near the antenna can affect its resonance performance. Since the battery is the largest among other components, we numerically simulated $|S_{11}|$ of the antenna at the center of the phantom for varying sizes of the battery, placed at the center of the capsule. The battery was modeled as a cylinder made of a perfect electric conductor with three different diameters of 7.5, 8.5 and 9 mm, while height was set to 7.2 mm. Results are shown in Fig. 3(d) indicating that for three sizes the resonance frequency of the antenna slightly increases compared to a hollow capsule. However, for the battery diameter of 7.5 and 8.5 mm, the antenna still maintained $|S_{11}|$ lower than -10 dB for a wide frequency range of about 1700 MHz.

C. Resonance, Radiation, Specific Absorption Rate (SAR) in a Realistic Human Body Model

Once a capsule is swallowed, it experiences a significant change of relative permittivity and conductivity depending on the surrounding tissues, such as, colon ($\varepsilon_\text{r} = 62$, $\sigma = 0.87$), stomach ($\varepsilon_\text{r} = 67.2$, $\sigma = 0.626$) and small intestine ($\varepsilon_\text{r} = 65.2$, $\sigma = 1.22$). Furthermore, the resonance and radiation characteristics of the ingestible antenna depend on the position of the capsule and surrounding tissues [22], [23], we therefore numerically studied these by simulating antenna with the 3-D CST Gustav voxel human body model. Note that due to the limited computing resources, only a human torso with the volume $290 \times 230 \times 100$ mm^3 was considered. When implanted in the colon, stomach, and small intestine, the capsule was 50, 90 and 85 mm away from the nearest body surface, respectively. Fig. 4 presents the simulated $|S_{11}|$ of the capsule antenna with a biocompatible layer for three tissues. The results demonstrate that for the proposed antenna $|S_{11}|$ is better than -10 dB at 433 MHz for all tissues and maintains a wider impedance matching bandwidth than any literature reports. The $\text{BW}_{-10\text{dB}}$ is enhanced when the antenna was in the small intestine, because of the low-quality factor of the antenna due to the highest $\tan\delta$ among other tissues. The simulated realized gain is -26.7, -28.2, and -33 dBi for the capsule antenna implanted in the colon, stomach, and small intestine, respectively. The antenna in small intestine shows a lower gain due to the higher conductivity compared to colon and stomach. It is worth mentioning that the gain is also affected by the distance from body surface as well as the size of the phantom.

Since the capsule antenna operates in a human body, radiation safety needs to be considered. One of the well-accepted radiation safety measures is the specific absorption ratio (SAR), which is the rate of energy deposited per unit mass of tissue. The IEEE C95.1-1999 [24] and C95.1-2005 [25] specify that 1-g and 10-g averaged SAR should be less than 1.6 W/kg and 2 W/kg, respectively. The maximum allowable input powers to the X-orientated capsule antenna have been numerically evaluated using the SAR calculator in CST Microwave Studio 2018 with the Gustav voxel model. The results show that the capsule antenna is safe to be used at the transmit power less than 4.3 and 25 mW in the colon,

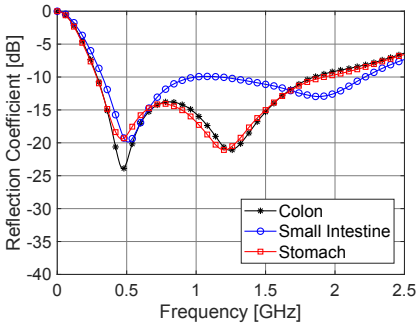

Fig. 4. Simulated reflection coefficient of the capsule antenna in CST Gustav voxel human body with three different tissue types, i.e., in colon, stomach and small intestine.

4.1 and 22.5 mW in the small intestine and 4.5 and 24 mW in the stomach for the 1-g and 10-g averaged SAR, respectively.

III. Antenna Fabrication and Measurements

The fabricated flat antenna before wrapping on the capsule module is presented in Fig. 5(a), whereas Fig. 5(b) shows it after wrapping on the outer surface of the pill. The details of the fabrication process are described in [26]. The capsule module is made of polystyrene with $\varepsilon_r = 2.6$ and $\tan\delta = 0.05$ at 1 GHz. The diameter and length of the capsule are 10 mm and 19.5 mm, respectively, whereas the thickness of the wall is 0.5 mm. After wrapping, points A and B in Fig. 5(a) were soldered together to form the loop so that the prototype was identical to the simulated design.

An illustration of the *in-vitro* measurement set-up for the antenna is presented in Fig. 6. The set-up included a vector network analyzer (VNA) and a rectangular-shaped plastic container, which was filled with a liquid mimicking the colon tissue. The liquid was formulated by mixing 79% salted water (7.85 g/L) and 21% TritonX-100. An HP 8720C network analyzer and 85070A dielectric probe kit were used to verify the electrical properties of the liquid phantom. The measured permittivity and loss tangent values at 433 MHz were 61.4 and 0.60, respectively, which are very close the values used in Section II-B. As to the feeding of the antenna, we used the similar method as presented in [17]. For differential feeding a wideband surface mount balun (Analen B0322J5050AHF) was used at the feeding point of the antenna in order to avoid the possible problem caused by the interaction between balanced antenna and unbalanced coaxial cable. The antenna was connected to the balanced ports of the balun, whereas center and outer conductors of the SMA connector were soldered to the unbalanced port and ground of the balun, respectively. During the measurements, we used a layer of sticky rubber with $\varepsilon_r = 2.2, \tan\delta = 5.0 \times 10^{-4}$ around the feeding components including balun, SMA connector, and coaxial cable to avoid the direct contact with the liquid. As the VNA was calibrated to the reference plane

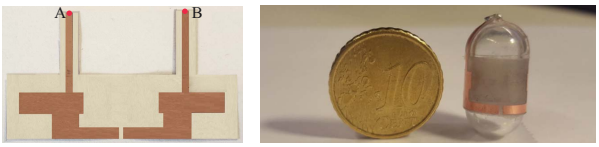

(a) (b)

Fig. 5. Fabricated capsule antenna (a) before (flat), and (b) after being wrapped onto the surface of the capsule module.

Fig. 6. Illustration of the *in-vitro* measurement setups.

of the SMA connector, the capsule antenna was also simulated with the SMA connector to test its impact on matching. We found a negligible impact on matching. The proposed capsule antenna was placed inside the colon-tissue liquid phantom as visualized in Fig. 6.

The comparison of the simulated and measured $|S_{11}|$ of an X-oriented capsule at the center of the liquid phantom is presented in Fig. 7. Note that the biocompatible layer and any components inside the capsule were not included in the measurement. The simulated plot is identical to the one in Fig. 3(a). The measurements agree well with the simulations, with only slight differences in the matching level, which might come from the fabrication process of the prototype. The measured $|S_{11}|$ of the proposed capsule antenna is better than -10 dB across the frequency range from 250 MHz to 1740 MHz, which agrees well with the simulated matching bandwidth. Thus the close agreement between simulation and measured results for this colon tissue case validates the robustness of proposed capsule antenna against different detuning factors. Table I shows a comparison of reported capsule antennas in the literature, designed frequencies are up to 1400 MHz. The matching bandwidth of the proposed capsule antenna is the widest among the existing solutions even though it utilizes much smaller capsule except [6], [10], which report much narrower matching bandwidth for a WCE system.

IV. Conclusion

In this paper, an ultrawideband conformal loop antenna is presented for a WCE system operating at 433 MHz. The antenna utilizes the outer-wall of the capsule module with a size of only 19.5 mm $\times$ 10 mm. Thus, the capsule size can be significantly reduced compared to existing WCE solutions. The proposed antenna shows a bandwidth $\text{BW}_{-10\text{dB}} = 1912$ MHz, i.e. from 288 to 2200 MHz. The proposed capsule antenna maintains the desired performance even if electronic modules are

TABLE I
A COMPARISON OF REPORTED CONFORMAL CAPSULE ANTENNAS IN THE LITERATURE, DESIGNED FREQUENCIES ARE UP TO 1400 MHZ: ANTENNA TYPE, OPERATING FREQUENCY,CAPSULE SIZE INCLUDING TWO DOMES, BW_{-10dB}, RADIATION PERFORMANCE IN THE REPORTED PHANTOM

Ref.	Antenna type	Frequency (MHz)	Capsule Size (mm)	Bandwidth (MHz)	Gain (dBi)	Phantom: tissue, shape, size (mm)
[6]	inner-wall microstrip	434	17×7	17	-22	Muscle, sphere, Ø100
[7]	outer-wall helix	433	30×10	20	-40.9	Muscle, cube, 190^3
[8]	outer-wall microstrip	402	28×11	39.9	-29.6	Muscle, cube, 100^3
[10]	microstrip	434	17×7	53	-33	$\varepsilon_r = 49.6, \sigma = 0.51$, cyl., Ø 200
[11]	inner-wall patch	433	25×12	124.4	-36.9	$\varepsilon_r = 56.4, \sigma = 0.82$, cyl. Ø 100 × 200
[12]	dipole	402	24×11	158	-37	Skin, cube, 180^3
[14]	inner-wall loop	915	26×11	185	-19.4	$\varepsilon_r = 55, \sigma = 0.95$ S/m, cube, 100^3
[15]	outer-wall dipole	1400	26×11	200	-26	Muscle, box, 350 × 350 × 200
[16]	inner-wall dipole	1400	26×11	200	-36	Muscle, box, 600 × 300 × 400
[17]	outer-wall loop	500	24×11	260		$\varepsilon_r = 56.4, \sigma = 0.82$, cyl. Ø150
[18]	outer-wall loop	500	21×11	785		$\varepsilon_r = 56.4, \sigma = 0.82$, box, 200 × 150 × 100
[19]	outer-wall loop	433	27×11	795	-35	Colon, box, 235 × 220 × 100
This paper	outer-wall loop	433	19.5×10	1912	-34.5	Colon, box, 235 × 220 × 100

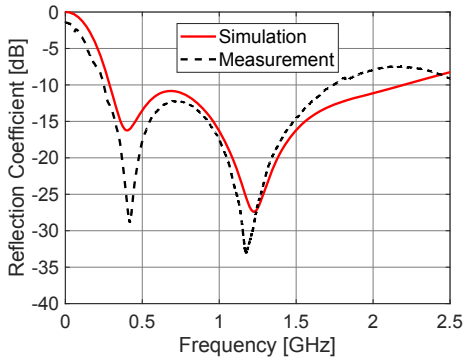

Fig. 7. Comparison of simulated and measured reflection coefficient: (a) X-oriented capsule antenna at the center of the phantom; the simulated curve is identical to the one in Fig. 3(a).

added into the capsule, and when the antenna is located at varying locations in the phantom, i.e., different tissues in the GI tract. With its very small size, ultrawide operational bandwidth and sufficient radiation performance, the proposed capsule antenna is especially suitable for pediatric patients, in addition to adult patients. Our future work includes evaluation of propagation losses between our proposed capsule antenna and an on-body receive antenna, and their link performance analysis, as well as a possible further capsule size reduction.

REFERENCES

[1] G. Iddan, G. Meron, A. Glukhovsky, and P. Swain, "Wireless capsule endoscopy," *Nature*, vol. 405, no. 6785, p. 417, May 2000.

[2] A. Khaleghi, M. S. E. Sendi, R. Chavez-Santiago, F. Mesiti, and I. Balasingham, "Exposure of the human brain to an electromagnetic plane wave in the 100-1000 MHz frequency range for potential treatment of neurodegenerative diseases," *IET Micro., Ant. Prop.*, vol. 6, no. 14, pp. 1565–1572, Nov. 2012.

[3] S. H. Lee, J. Lee, Y. J. Yoon, S. Park, C. Cheon, K. Kim, and S. Nam, "A wideband spiral antenna for ingestible capsule endoscope systems: Experimental results in a human phantom and a pig," *IEEE Trans. on Bio. Eng.*, vol. 58, no. 6, pp. 1734–1741, June 2011.

[4] S. H. Lee and Y. J. Yoon, "A dual spiral antenna for ultra-wideband capsule endoscope system," in *Int. Workshop on Ant. Tech.: Small Antennas and Novel Metamaterials*, Mar. 2008, pp. 227–230.

[5] V. Shirvante, F. Todeschini, X. Cheng, and Y. K. Yoon, "Compact spiral antennas for mics band wireless endoscope toward pediatric applications," in *IEEE Ant. and Propag. Soc. Int. Sym.*, July 2010, pp. 1–4.

[6] D. Nikolayev, M. Zhadobov, L. L. Coq, P. Karban, and R. Sauleau, "Robust ultraminiature capsule antenna for ingestible and implantable applications," *IEEE Tran. on Ant. and Prop.*, vol. 65, no. 11, pp. 6107–6119, Nov. 2017.

[7] J. Faerber, G. Cummins, S. K. Pavuluri, P. Record, A. R. A. Rodriguez, H. S. Lay, R. McPhillips, B. F. Cox, C. Connor, R. Gregson, R. E. Clutton, S. R. Khan, S. Cochran, and M. P. Y. Desmulliez, "In vivo characterization of a wireless telemetry module for a capsule endoscopy system utilizing a conformal antenna," *IEEE Trans. on Bio. Cir. and Sys.*, vol. PP, no. 99, pp. 1–11, 2017.

[8] A. Konstantinos, A. Kiourti, and K. Nikita, "A novel conformal antenna for ingestible capsule endoscopy in the MedRadio band," in *Prog. in Elec. Res. Sym. Proc.*, Stockholm, Sweden, Aug. 2013.

[9] X. Cheng, J. Wu, R. Blank, D. E. Senior, and Y. K. Yoon, "An omnidirectional wrappable compact patch antenna for wireless endoscope applications," *IEEE Ant. and Wireless Prop. Let.*, vol. 11, pp. 1667–1670, 2012.

[10] Y. Mahe, A. Chousseaud, M. Brunet, and B. Froppier, "New flexible medical compact antenna: Design and analysis," *Int. J. Ant. and Prop.*, vol. 2012, no. 837230, p. 6 pages, 2012.

[11] M. S. Arefin, J. M. Redoute, and M. R. Yuce, "Meandered conformal antenna for ISM-band ingestible capsule communication systems," in *38th Annual Int. Conf. of the IEEE Eng. in Med. and Bio. Soc. (EMBC)*, Aug. 2016, pp. 3031–3034.

[12] L. J. Xu, Y. X. Guo, and W. Wu, "Bandwidth enhancement of an implantable antenna," *IEEE Ant. and Wireless Prop. Let.*, vol. 14, pp. 1510–1513, 2015.

[13] K. Kwon, W. Seo, S. Lee, and J. Choi, "Design of an antenna for an ingestible capsule endoscope system," in *3rd IEEE International Conference on Network Infrastructure and Digital Content*, Sept. 2012, pp. 62–65.

[14] R. Das and H. Yoo, "A wideband circularly polarized conformal endoscopic antenna system for high-speed data transfer," *IEEE Tran. on Ant. and Prop.*, vol. 65, no. 6, pp. 2816–2826, June 2017.

[15] P. Izdebski, H. Rajagopalan, and Y. Rahmat-Samii, "Conformal ingestible capsule antenna: A novel chandelier meandered design," *IEEE Trans. Ant. Prop.*, vol. 57, no. 4, pp. 900–909, Apr. 2009.

[16] H. Rajagopalan and Y. Rahmat-Samii, "Wireless medical telemetry characterization for ingestible capsule antenna designs," *IEEE Ant. and Wireless Prop. Let.*, vol. 11, pp. 1679–1682, 2012.
[17] Y. Sumin, K. Kihyun, and N. Sangwook, "Outer-wall loop antenna for ultrawideband capsule endoscope system," *IEEE Ant. Wireless Prop. Letters.*, vol. 9, pp. 1135–1138, 2010.
[18] R. Alrawashdeh, Y. Huang, and G. Ping C.and Eng, "A new small conformal antenna for capsule endoscopy," in *7th European Conf. on Ant. Prop. (EuCAP 2013)*, Gothenburg, Sweden, Apr. 2013, pp. 220–223.
[19] M. S. Miah, A. N. Khan, C. Icheln, K. Haneda, and K. I. Takizawa, "Antenna systems for wireless capsule endoscope: Design, analysis and experimental validation," *IEEE Trans. Ant. and Propag.*, pp. 1–11, 2018. [Online]. Available: availableatarXive-prints,http://arxiv.org/abs/1804.01577
[20] R. Shamir and R. Eliakim, "Capsule endoscopy in pediatric patients," *World J of Gastroenterology*, vol. 14, no. 26, pp. 4152–4155, July 2008.
[21] B. Antao, J. Bishop, R. Shawis, and M. Thomson, "Clinical application and diagnostic yield of wireless capsule endoscopy in children," *J Laparoendosc Adv. Surg. Tech. A*, vol. 17, no. 3, pp. 364–370, June 2007.
[22] L. Xu, M. Q. H. Meng, and Y. Chan, "Effects of dielectric parameters of human body on radiation characteristics of ingestible wireless device at operating frequency of 430 MHz," *IEEE Trans. on Bio. Eng.*, vol. 56, no. 8, pp. 2083–2094, Aug. 2009.
[23] L. C. Chirwa, P. A. Hammond, S. Roy, and D. R. S. Cumming, "Radiation from ingested wireless devices in biomedical telemetry bands," *Elect. Let.*, vol. 39, no. 2, pp. 178–179, Jan. 2003.
[24] "IEEE standard for safety levels with respect to human exposure to radio frequency electromagnetic fields, 3 KHz to 300 GHz," *IEEE Standard C95.1-1999*, 1999.
[25] "IEEE standard for safety levels with respect to human exposure to radio frequency electromagnetic fields, 3 KHz to 300 GHz," *IEEE Standard C95.1-2005*, 2005.
[26] M. S. Miah, K. Haneda, C. Icheln, A. Khatun, and K. I. Takizawa, "An ultrawideband conformal loop antenna for ingestible capsule endoscope system," in *10th European Conf. on Ant. and Prop. (EuCAP 2016)*, Apr. 2016, pp. 1–5.